Biomimetic Intelligence and Robotics 4 (2024) 100183

Contents lists available at ScienceDirect

Biomimetic Intelligence and Robotics

journal homepage: www.elsevier.com/locate/birob

Research Article

Human–robot collaborative handling of curtain walls using dynamic motion primitives and real-time human intention recognition

Fengming Li [a], Huayan Sun [a], Enguang Liu [b,*], Fuxin Du [c]

[a] School of Information and Electrical Engineering, Shandong Jianzhu University, Jinan 250101, China
[b] Shandong Transportation Institute, Jinan 250031, China
[c] School of Mechanical Engineering, Shandong University, Jinan 250012, China

ARTICLE INFO

Article history:
Received 30 April 2024
Revised 12 July 2024
Accepted 26 August 2024
Available online 10 September 2024

Keywords:
Robots
Dynamic motion primitives
Human–machine collaboration
Curtain wall handling

ABSTRACT

Human–robot collaboration fully leverages the strengths of both humans and robots, which is crucial for handling large, heavy objects at construction sites. To address the challenges of human–machine cooperation in handling large-scale, heavy objects — specifically building curtain walls — a human–robot collaboration system was designed based on the concept of "human–centered with machine support". This system allows the handling of curtain walls according to different human intentions. First, a robot trajectory learning and generalization model based on dynamic motion primitives was developed. The operator's motion intent was then characterized by their speed, force, and torque, with the force impulse introduced to define the operator's intentions for acceleration and deceleration. Finally, a collaborative experiment was conducted on an experimental platform to validate the robot's understanding of human handling intentions and to verify its ability to handle curtain wall. Collaboration between humans and robots ensured a smooth and labor-saving handling process.

1. Introduction

In the assembly of building curtain walls, the complex environmental constraints of construction sites often require multiple workers to manually complete the assembly process [1]. Robots are an ideal solution for such tasks, and it has become an inevitable trend to introduce robots to replace traditional handling methods.

Traditional robot handling of objects typically involves writing complex programs in advance to guide the robot through the task. Although this approach can manage basic handling operations, it often falls short in complex scenarios and tasks. Teaching robots to learn handling skills [2] are flexible and intelligent alternative. Robot skill–learning is often achieved through reinforcement learning [3,4]. However, reinforcement learning for assembly tasks has limitations, such as slow convergence and lengthy computation times. As a result, researchers have increasingly explored imitation learning [5–7]. Several theories have been widely applied in human–machine skill transfer tasks, including the Gaussian Mixture Model (GMM) [8,9], Hidden Markov Models (HMM) [10], and Dynamic Motion Primitives (DMP) [11]. The GMM learns the probabilistic features of multiple training samples, including time-based and multidimensional inputs. The HMM is effective for learning various types of trajectories and is often used for skill reproduction. However, GMM and HMM struggle to generalize training trajectories to new situations. In contrast, the DMP theory offers stronger generalization capabilities than GMM and HMM [12,13]. Due to its flexibility, superior learning, and generalization abilities, DMP has been widely used to address the robot skill–learning problem.

However, handling skill–learning often prioritizes the robot's end-effector position optimization while neglecting speed optimization during movement [14]. Therefore, it is necessary to understand the operator's intentions during the handling process. Additionally, in real-world cooperative transport, operator intentions can change based on the operating environment, task conditions, and other influencing factors. The key to effective human–machine collaboration lies in the robot's ability to interpret the operator's motion intentions through sensor data [15,16]. Traditional force–displacement relationships only provide a simplistic definition of the operator's intentions, leading to issues like limited information, slow response times, and inappropriate motion speeds, which increase the risk of damage to the transported object [17]. Therefore, the robot system must be capable of learning and understanding a human's actual target intentions to successfully perform cooperative handling tasks. The robot should dynamically adapt to changes in intention in real time during the skill model's generalization. By integrating intention recognition [18,19] into the skill–learning process, the robot can accurately and quickly follow the operator's intentions,

* Corresponding author.
E-mail address: leg61908394@foxmail.com (E. Liu).

https://doi.org/10.1016/j.birob.2024.100183

allowing real-time adjustments to the speed of movement. Thus, defining and accurately understanding human intentions is a critical challenge when robots are learning human handling skills.

This study aims to design a human–robot collaborative curtain wall handling system using a skill–learning method. Based on the concept of "human-centered with machine support" the robot serves as the primary load-bearing unit and is guided by an operator to facilitate curtain wall handling. The operator's intentions are detected through a force sensor, and speed control during skill–learning is achieved by integrating a generalization model based on DMP. This approach enhances the stability of the control system and the flexibility of collaborative work, ensuring that the robot operates smoothly and responsively, thereby making the curtain wall handling process more efficient and labor-saving. The primary contributions of this article are as follows:

(1) A robot system suitable for human–robot cooperative handling is developed based on the "human-centered with machine support" model.
(2) A robot handling skill–learning method based on the DMP algorithm is proposed to establish a trajectory learning and generalization model for the curtain wall handling robot. This model enables the learning of curtain wall handling skills and allows for the planning of new motion trajectories based on the teaching trajectory and new start and end points.
(3) The operator's intentions are described by changes in the robot's movement speed, the force applied by the operator, and variations in the impulse. Intention recognition is integrated into the skill–learning process to allow real-time speed adjustments, thereby ensuring that human–robot curtain wall handling is safer and less labor-intensive.

The remainder of this paper is organized as follows: Section 2 describes the handling system composition. Section 3 describes the proposed method. The experiments and results are presented in Section 4, and the conclusions are drawn in Section 5.

2. System description

In human–robot collaborative handling operations, variability in human operators' intentions can introduce uncertainty, leading to unstable robot movements. A key challenge is to accurately describe and understand human intentions so that robots can effectively and smoothly handle heavy objects in a collaborative setting. This paper focuses on building facades as targets for operations and designs a human–robot collaborative handling system aimed at achieving facade handling tasks through real-time trajectory planning based on an understanding of human intentions.

Fig. 1 illustrates the human–machine collaborative curtain wall handling system. The blue lines represent the integration of human intentions with the robot's trajectory model. The orange lines indicate the integration of the target's initial and final points with the trajectory learning model. The orange lines also show data collected from the force sensor and robot, while the blue line shows the process of generating instructions for the robot. The computer uses the information collected from the force sensor and robot to interpret human intentions, and it uses data on the teaching trajectories and starting and ending points to learn and plan the trajectory. The system comprises three primary modules: the intent understanding module, executive module, and motion trajectory planning module.

The intent understanding module collects real-time force data from human gripping actions on the curtain wall using a six-axis force sensor. The module also reads the motion information of the robot end effector to estimate whether the current human intention is to accelerate, decelerate, or maintain the current speed. The sensors are installed on the curtain wall. A Kalman filtering algorithm is applied to the force sensor data to smooth out the force curves. The motion trajectory planning module generates robot motion trajectories at various speeds using trajectory learning and generalization models. The executive module integrates real-time human intentions with the motion trajectories to dynamically plan new trajectories, thereby facilitating the assembly of the curtain wall.

3. Method

3.1. Framework for skill–learning by the robot

The robot handling process with the operator is illustrated in Fig. 2. The proposed framework includes robot trajectory learning and generalization based on DMP and human intention understanding.

During the learning phase, the robot fits the nonlinear control terms f using the recorded motion trajectories and obtains the corresponding weight parameters w. The starting and target poses are specified for trajectory generalization. The learned weight parameters w are then incorporated into a nonlinear function approximation equation to plan a new motion trajectory. The robot interprets human intentions during the teaching process and integrates generalized trajectories at different speeds to plan a new movement trajectory. This approach allows the robot to perform cooperative handling tasks more efficiently and safely along the new trajectory.

3.2. Robot trajectory learning and generalization

In human–robot collaborative handling, the robot models complex trajectories with a small set of parameters and generalizes them by adjusting task parameters to expand its operational skills for new environments. To enable the robot trajectory learning model to fit various trajectory shapes, a nonlinear control term including time is added to modify the trajectory based on the core dynamic system of the DMP algorithm. This adjustment addresses the system's nonlinearity. The proposed robot trajectory learning and generalization model are illustrated in Fig. 3.

In this model, the robot's end pose is set as the state variable, the target pose is the state attractor, and a radial basis function network is used to describe the nonlinear control term. As shown in Eqs. (1) and (2):

$$f_p(t) = \frac{\sum_{i=1}^{M} \omega_{i,p} \Psi_i(t)}{\sum_{i=1}^{M} \Psi_i(t)} \tag{1}$$

$$f_q(t) = \frac{\sum_{i=1}^{M} \omega_{i,q} \Psi_i(t)}{\sum_{i=1}^{M} \Psi_i(t)} \tag{2}$$

As shown above, p and q represent the end displacement and rotational angle of the robot, i represent the number of radial basis functions, The parameters $\omega_{i,p}$ and $\omega_{i,q}$ denote the weight parameters, $f_p(t)$ and $f_q(t)$ denote the nonlinear forcing terms associated with translation and rotation, respectively.

By combining M radial basis functions according to their different weights to form nonlinear functions, the system model learns and approximates any desired trajectory shape. The parameters $\omega_{i,p}$ and $\omega_{i,q}$ represent the weights of the radial basis function at the sampling point. Through a regression analysis of the collected teaching trajectory and the assignment of each weight, the robot trajectory during transport is constructed. The radial basis function [20] is the Gaussian function for Eq. (3):

$$\Psi_i(t) = \exp\left(-h_i (t - c_i)^2\right) \tag{3}$$

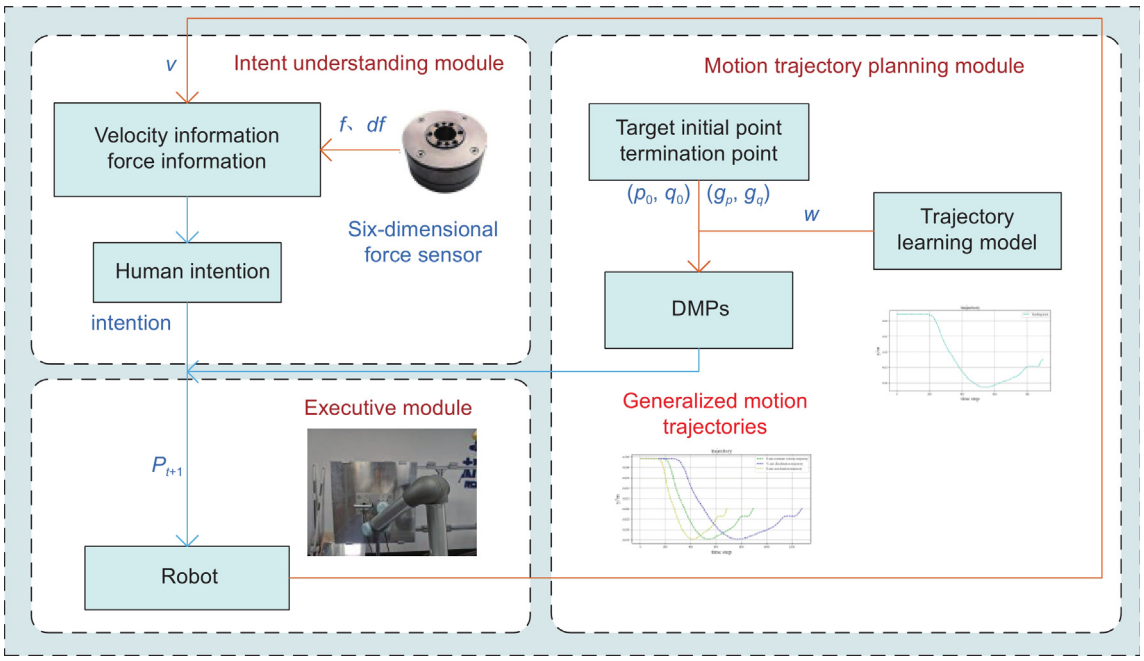

Fig. 1. Human–machine collaborative curtain wall handling system.

The parameters $\omega_{i,p}$ and $\omega_{i,q}$, represent the weights of the radial basis function at the sampling point; $\Psi_i(t)$ denotes the radial basis function; c_i and h_i are the central position and width of the basis function, respectively. Each Gaussian kernel function should be evenly distributed along the time axis. When the number of radial basis functions is adequate, any complex trajectory can be fitted by adjusting the center position of each basis function, the width of the basis function, and its participation weight.

To ensure that trajectories having multiple degrees of freedom are synchronized in time with the control system, a phase quantity x that is independent of time is used instead of time t, and the nonlinear forcing terms are rewritten as the separate phase state functions $f_p(x)$ and $f_q(x)$.

At the same time, the position and attitude of the starting point are also considered as factors that affect the nonlinear forcing term p_0, and q_0 represents the starting state of the robot, given that the fitting effect of the nonlinear forcing term is poor when the difference between the initial point and the target point is too little. The nonlinear forcing terms are shown in Eqs. (4) to (7):

$$x = e^{-\frac{\alpha_x}{\tau}t} \tag{4}$$

$$\tau\dot{x} = -\alpha_x x \tag{5}$$

$$f_p(x) = \frac{\sum_M^{i=1}\omega_{i,p}\Psi_i(x)}{\sum_M^{i-1}\Psi_i(x)}x(p - p_0) \tag{6}$$

$$f_q(x) = \frac{\sum_M^{i=1}\omega_{i,q}\Psi_i(x)}{\sum_M^{i-1}\Psi_i(x)}x(q - q_0) \tag{7}$$

The learning model for the robot handling trajectory is then expressed as Eq. (8):

$$\begin{bmatrix}\dot{z}\\ \dot{p}\\ \dot{\varphi}\\ \dot{q}\\ \dot{x}\end{bmatrix} = \begin{bmatrix}\left(\alpha_z\left(\beta_z\left(g_p - p\right) - z\right) + f_p(x)\right)/\tau\\ z/\tau\\ \left(\alpha_z\left(\beta_z 2\log\left(g_p * \bar{q}\right) - \varphi\right) + f_p(x)\right)/\tau\\ \frac{1}{2}\varphi * q\\ -\alpha_x x/\tau\end{bmatrix} \tag{8}$$

To improve the adaptability of the robot to a variety of handling tasks, the trajectory is generalized to different starting points, different ending points, and different traveling speeds of the robot during movement. First, the motion features are fitted based on the model parameters learned from the collected demonstration curtain wall transportation track sample data so as to generalize to different starting points and ending points. This is done by setting the new starting point pose p_0 and q_0 with the target end point pose g_p and g_q. The corresponding weights for each radial basis function are then obtained to establish the nonlinear forcing terms. Second, the variation of speed during the handling process is transformed into the effect of regular system parameters, and a factor ∂ for the speed effect is added to change the phase attenuation amplitude to realize trajectory generalization. The factor for the effect of speed is given as Eq. (9):

$$\dot{x} = -\frac{\alpha_x x}{\partial\tau} \tag{9}$$

The factor for scaling speed is denoted as

$$\partial = r + \frac{\sum_{i=1}^{K}\partial_i\Psi_i(x)}{\sum_{i=1}^{K}\Psi_i(x)} \tag{10}$$

where r is a constant, ∂_i is a weight and $\Psi_i(x)$ is a radial basis function. α_x is a gain parameter, τ is a time constant. Parameters α_x, ∂ and τ in Eq. (9) affect the speed in trajectory generalization. By adjusting the values of these parameters, trajectories with different speeds can be generated to meet the needs. At the robot trajectory learning stage, the external force term f is modeled based on the robot motion trajectory demonstration data, so as to obtain the corresponding weight parameters. After the new starting and ending points are specified, the learned weight parameters ω are brought into an equation to approximate a nonlinear function by resetting the canonical system, and a new transport trajectory is planned.

3.3. Understanding human intent

The intent understanding module is a critical component of the human–robot collaborative handling system. The robots interact with humans through this module by using sensors to collect

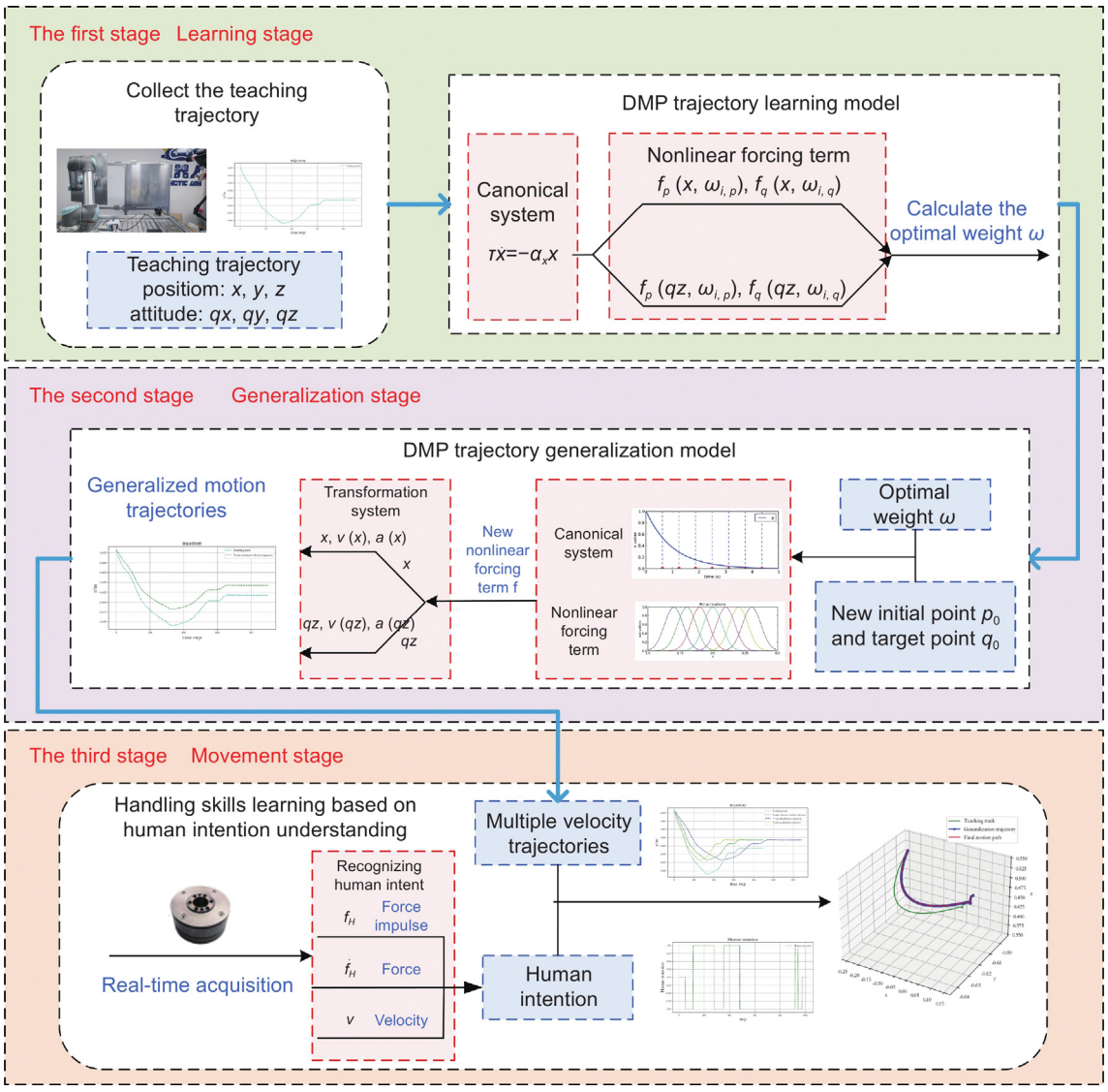

Fig. 2. Framework of the robot handling process with the operator.

and understand the operator's work intentions. These intentions then transformed into robot actions to effectively complete the collaborative processing tasks. In this study, we propose a better definition of operator intent by analyzing changes in the speed of the robot and the variations in the forces and force impulses exerted by operators during the collaboration.

The collaborative handling task described in this paper is divided into three distinct phases: initiation, operation, and termination, as illustrated in Fig. 4. During the initiation phase, the operator's intention is to initiate the collaborative handling process and accelerate it from a standstill. In this phase, the operator applies a force, and the impulse (the first derivative of the applied force f) aligns with the object's velocity v. Once the robot's speed exceeds 0.25 m/s, it transitions into the operation phase. Here, the robot must recognize the operator's acceleration or deceleration intentions in real time and generate new motion trajectories accordingly. The impulse defines the operator's acceleration and deceleration intentions. In the termination phase, the operator attempts to stop the cooperative handling process and bring the robot's speed to zero. During this phase, the operator applies force and impulse in the direction opposite to the object's velocity v.

The process is governed by the equation shown in Eq. (11):

$$\begin{cases} v * df_H > 0 \;\Rightarrow\; \begin{cases} v * f_H > 0 \\ v * f_H < 0 \end{cases} \\ \qquad\qquad \Rightarrow \begin{cases} \textit{Operator intention: accelerate} \\ \textit{Operator intention: decelerate} \end{cases} \\ v * df_H < 0 \;\Rightarrow\; \textit{Operator intention: decelerate} \\ v * df_H \approx 0 \;\Rightarrow\; \textit{Operator intention: constant} \end{cases} \tag{11}$$

where v represents the robot's end-movement speed, f_H denotes the force applied by the operator, and df_H is the force impulse (i.e., the first derivative of the applied force f_H). The operator's intention is categorized as acceleration, deceleration, or constant speed. By modifying the parameters of the canonical system in DMP, the convergence rate of the system can be adjusted to generalize the trajectories at different speeds between the starting and ending points. When the robot's end-movement speed and applied force are below a threshold, the system defines this period as either the start or end stage, and the next point is planned based on the original speed trajectory. During the operation phase, if the product of the speed and force impulse is below the threshold, the motion is considered to be at the original speed, and the next point follows the original speed trajectory.

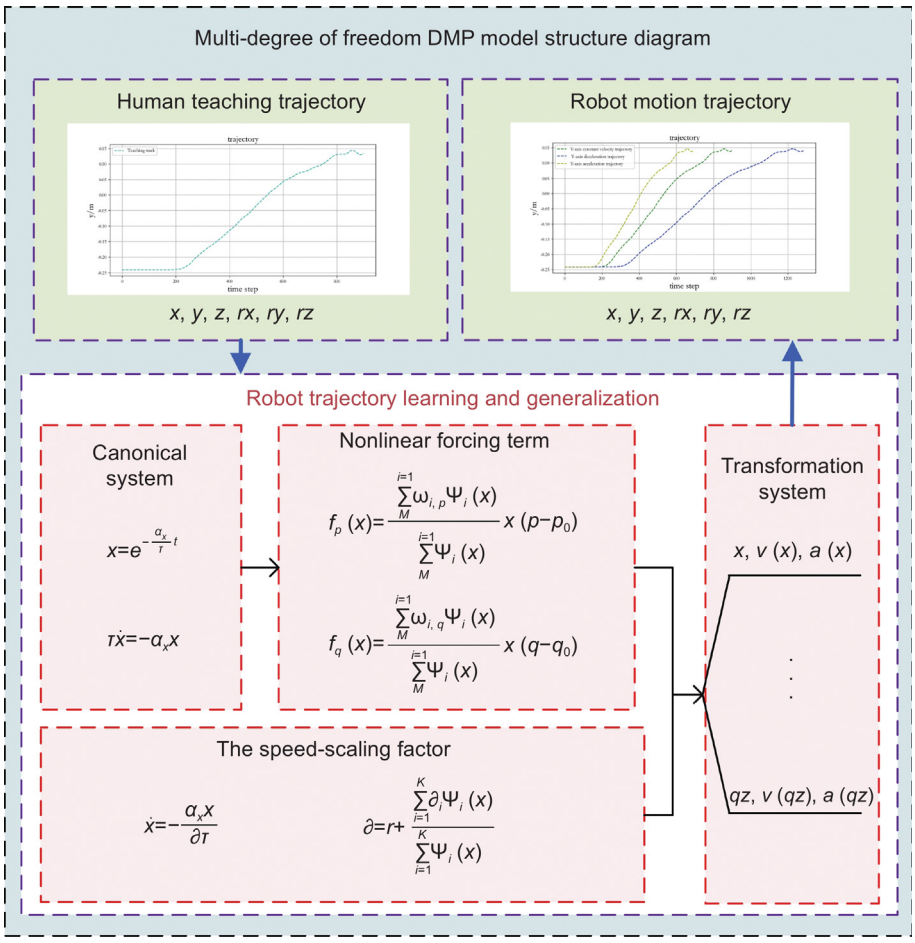

Fig. 3. Structure of the multidegree-of-freedom dynamic motion primitive (DMP) model.

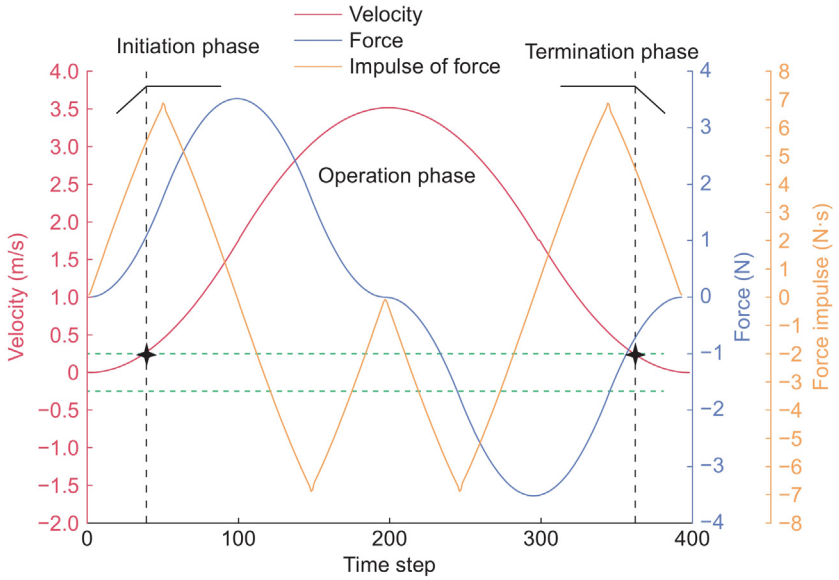

Fig. 4. Diagram showing the segmentation of the collaborative task.

If the product of speed and force impulse exceeds the threshold and aligns with the direction of velocity, the motion is defined as acceleration, and the next point is planned according to the acceleration trajectory. Conversely, if the product is above the threshold but opposite in direction, the motion is decelerated, and the next point is planned according to the deceleration trajectory. By collecting real-time intent data, three generalized trajectories with different speeds are connected to create a smoother and more suitable trajectory, enabling more precise and safer control skill–learning.

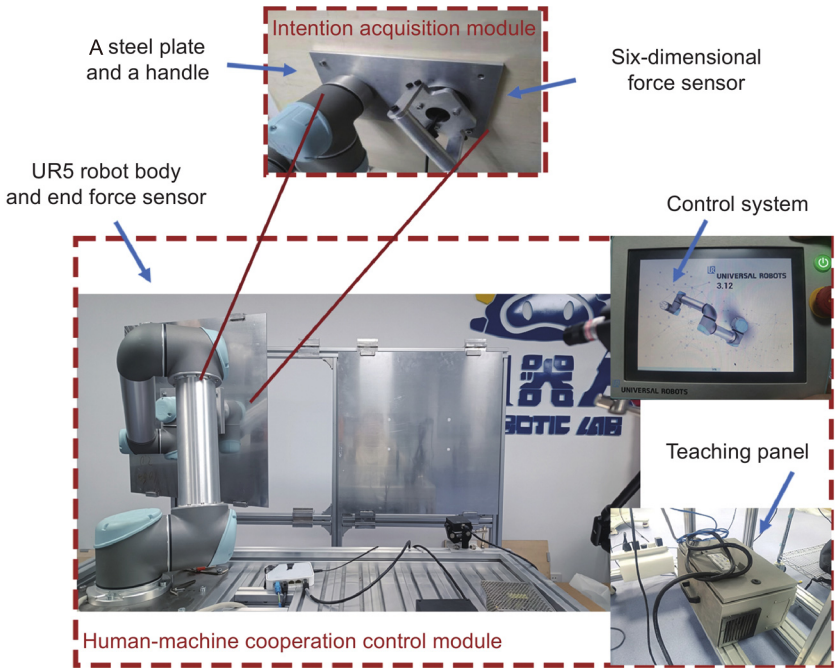

Fig. 5. Experimental platform.

4. Experiment

4.1. Construction of experimental platform

Fig. 5 illustrates the experimental system for curtain wall human–machine cooperative robot handling that was built for this study. This system includes the intent acquisition module and the human–machine cooperation control module.

The intention acquisition module includes a six-dimensional force sensor, a steel plate, and a handle. The force sensor detects both the magnitude and direction of the force applied by the operator, which is transmitted to the computer via cables. The upper computer then calculates and sends motion instructions to the curtain wall-handling robot. The six-dimensional force sensor used is the M4313M4B model from Sunrise Instruments, while the UR5 robot is used for the handling tasks. The UR5 robot is a collaborative robot from Universal Robots. The human–machine cooperation control module consists of the UR5 robot body, an end force sensor, a control system, and a teaching panel. During collaborative handling, the robot gathers information from the operator via a force sensor to interpret human intentions. The robot communicates with the computer through a serial port and executes motion instructions based on the planned trajectories, integrating human intentions into the collaborative handling process. The end-load capacity determines the maximum weight the UR5 robot can safely handle without compromising its stability or safety. Due to the UR5 robot's maximum end-load capacity of 5 kg, a steel curtain wall with a side length of 80 cm is used in place of a stone curtain wall for the experiments.

4.2. Robot trajectory learning and trajectory generalization experiment

To assess the effectiveness of robot trajectory learning and generalization, the robot's movement along a given target path was tested on the platform. Fig. 6 depicts the robot's teaching trajectory, with the preset starting point at (−0.126751, −0.630049, 0.510334) and the ending point at (0.142561, −0.62661, 0.510393), which were used to build the trajectory learning model.

Table 1
Trajectory planning experimental data: Fixed starting point and changing ending point.

Serial number	Target ending point	Actual ending point	Error
1	(0.06845, −0.42873, 0.34407)	(0.06797, −0.42915, 0.34397)	0.277%
2	(0.08845, −0.41373, 0.35407)	(0.08801, −0.41410, 0.35396)	0.152%
3	(0.09345, −0.41873, 0.33907)	(0.09302, −0.41912, 0.33898)	0.097%

First, the position of the starting point (x, y, z) is fixed, and the target points are set to (0.122561, −0.61661, 0.510393), (0.192561, −0.61661, 0.510393), and (0.242561, −0.63161, 0.505393). We calculate the trajectory of the transformed target point, and we calculate the error according to Eq. (12). We then verify the efficiencies of the robot learning and generalization.

$$erro = \frac{dis\,(\text{target point} - \text{actual point})}{dis\,(\text{target point} - \text{original point})} \times 100\% \tag{12}$$

where *erro* is the defined experimental error, and *dis* is the Euclidean distance between two points. The experimental results are summarized in Table 1 and Fig. 7. The data indicate that the trajectory learning model effectively learns and reproduces the teaching trajectory, with a generalization error of less than 0.278%, demonstrating the model's high accuracy and effectiveness in trajectory learning and generalization.

Secondly, we assigned the target point (0.27845, −0.42373, 0.34907) to a constant value, and we chose three different starting points: (0.32818, −0.26397, 0.22901), (0.22818, −0.28396, 0.19901), and (0.29818, −0.25397, 0.26901). Experimental results are shown in Table 2 and Fig. 8. As can be seen from the Table 2, the experimental error is less than 0.0001%. The robot motion trajectories that were learned maintained the same trend as similar teaching trajectories. The error rate is low, which verifies the effectiveness of the model. The experimental results are shown in Table 2 and Fig. 8, which indicate that the experimental error is less than 0.0001%.

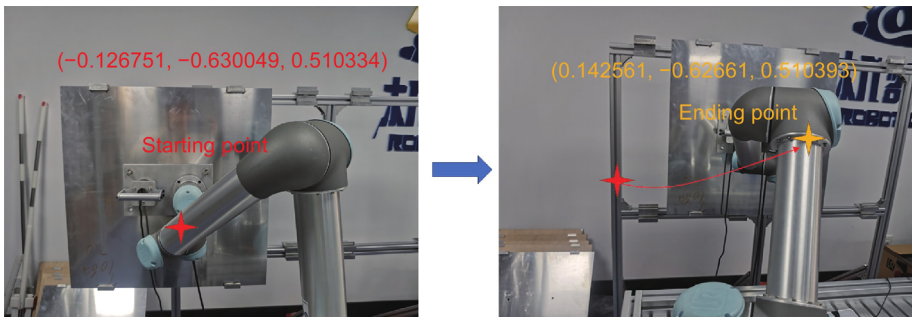

Fig. 6. Robot teaching trajectory.

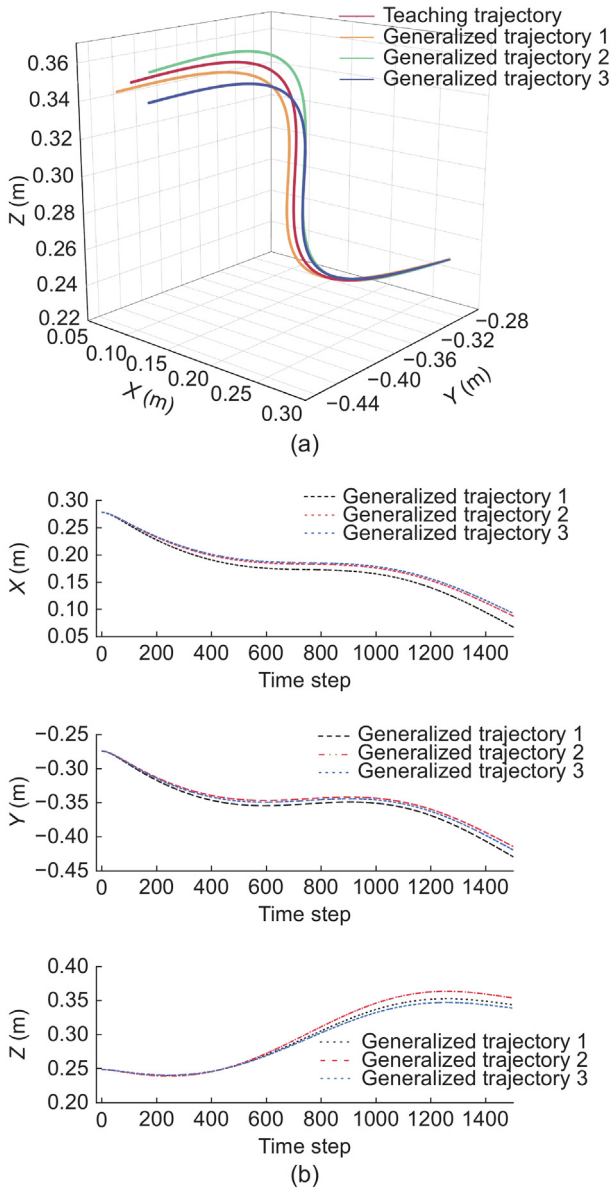

Fig. 7. Fixed starting point change ending point trajectory planning experiment. (a) Trajectory in three-dimensional space. (b) Trajectory for each dimension.

Finally, different starting points and target points are set, and the experimental results obtained are shown in Table 3 and Fig. 9. As can be seen from Table 3, the error of the motion trajectory generated through robot trajectory learning and the reproduction model are both less than 0.07%, and the maximum is 0.0622%, which indicates small error. The robot motion trajectories that were learned in the figure maintain the same trend as similar teaching trajectories. The error rate is low, which verifies the effectiveness of the model.

Table 2
Trajectory planning experimental data: Fixed ending point change starting point.

Serial number	Target starting point	Actual starting point	Error
1	(0.32819, −0.26396, 0.22901)	(0.32818, −0.26397, 0.22901)	0.0000958%
2	(0.22819, −0.28396, 0.19901)	(0.22818, −0.28396, 0.19901)	0.0000304%
3	(0.29819, −0.25396, 0.26901)	(0.29818, −0.25397, 0.26901)	0.0000212%

4.3. Human–machine cooperative handling experiment

To verify the robot's ability to recognize human intentions during curtain wall transportation, we assumed that human intentions were presupposed on the experimental platform shown in Fig. 5. During the experiment, information about the operator under the conditions of acceleration, deceleration, and constant speed was collected, including the operator's applied force, impulse, and robot end speed, to represent the operator's current motion intention (see Fig. 10).

First, the experiment for linear motion in human–machine cooperative space was carried out. In the simulation of the curtain wall assembly process, the operator puts the robot in the acceleration process when the distance from the installation target point is far. When the robot is approaching the target point, the operator puts the robot in the deceleration process. During the operation phase, we expect that the intention is to accelerate and decelerate. Linear movement in the X, Y, and Z directions is carried out. In the X direction, the curtain wall moves from the starting point (−0.23978) to the ending point (0.01566). Along the Y-axis, the curtain wall moves from the starting point (−0.59582) to the ending point (−0.644216). In the Z direction, the curtain wall moves from the starting point (0.50989) to the ending point (0.51022). The motion trajectory of the robot during the process of linear transport is obtained as shown in Fig. 9. A change in human intention occurred at time points 167, 130, and 190. The time points are measured in units of 1/150 s. The motion trajectories of the X, Y, and Z axes show a trend of initial acceleration, followed by deceleration. During the acceleration phase, the generated trajectory generally coincides with the accelerated trajectory. After the intention has changed to deceleration, the displacement trend of the generated trajectory is similar to that of the deceleration trajectory. It is shown that the errors of the three generated trajectories are 0.03377, 0.02377, and 0.2250, which

Table 3
Trajectory planning experimental data: changing starting point and ending point.

Serial number	Target starting and ending points	Actual starting and ending points	Error
1	(0.32818, −0.26396, 0.29901)/ (0.08790, −0.40410, 0.37899)	(0.32819, −0.26396, 0.29901)/ (0.08845, −0.40373, 0.37907)	0.00435%
2	(0.238186, −0.29396, 0.22901)/ (0.05804, −0.42408, 0.38890)	(0.23819, −0.29396, 0.22901)/ (0.05845, −0.42373, 0.38907)	0.00761%
3	(0.30818, −0.27396, 0.24601) (0.05787, −0.40408, 0.36894)	(0.30819, −0.27396, 0.24601)/ (0.05845, −0.40373, 0.36907)	0.0622%

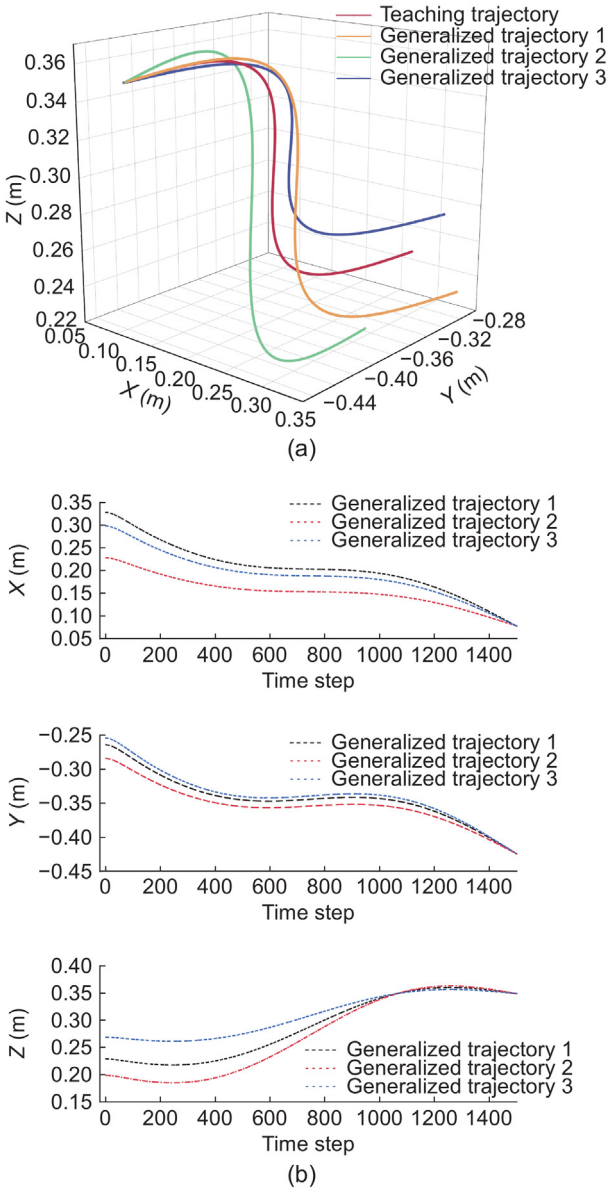

Fig. 8. Fixed ending point change starting point experiment. (a) Trajectory in three-dimensional space. (b) Trajectory for each dimension.

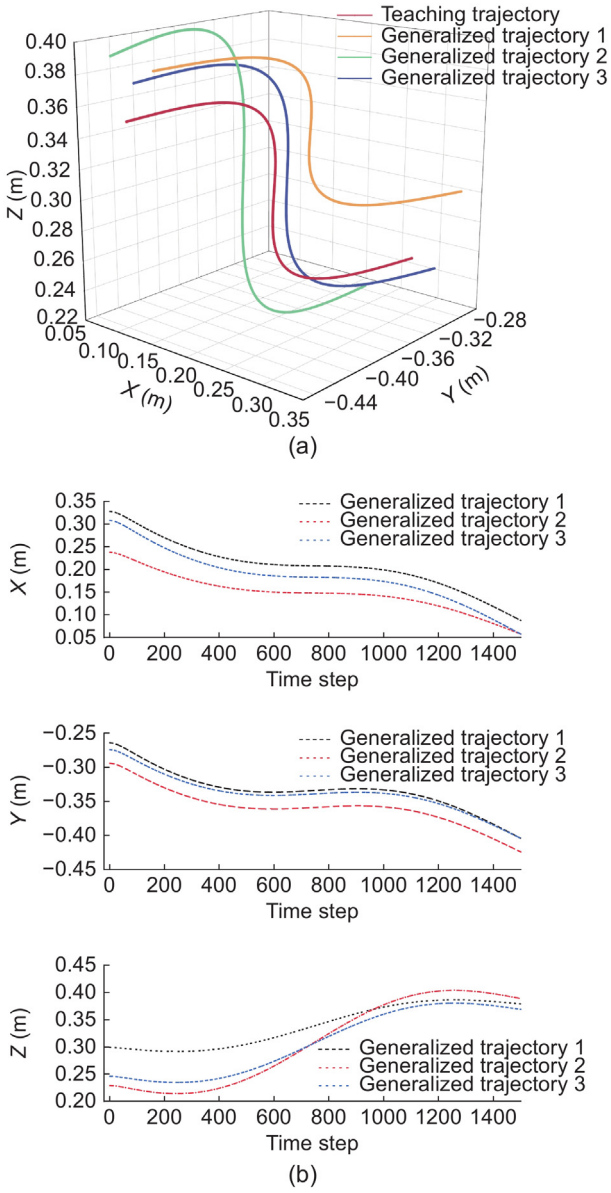

Fig. 9. The starting and ending points change the experiment. (a) Trajectory in three-dimensional space. (b) Trajectory for each dimension.

meet requirements. It can be seen from the experiment that the motion trajectory of each axis is divided into two parts: the first part shows the same trend as the acceleration trajectory, and the second part shows the same trend as the deceleration trajectory. The robot recognizes the acceleration and deceleration intentions during the motion stage.

During the building construction process, curtain wall handling is not a straight-line movement, so a transport experiment with multidirectional and curved movement in space is set up to verify the accuracy of the robot's understanding of the intention.

We simulated the experiment of human - machine cooperation to transport a curtain wall from the starting point (0.27820,

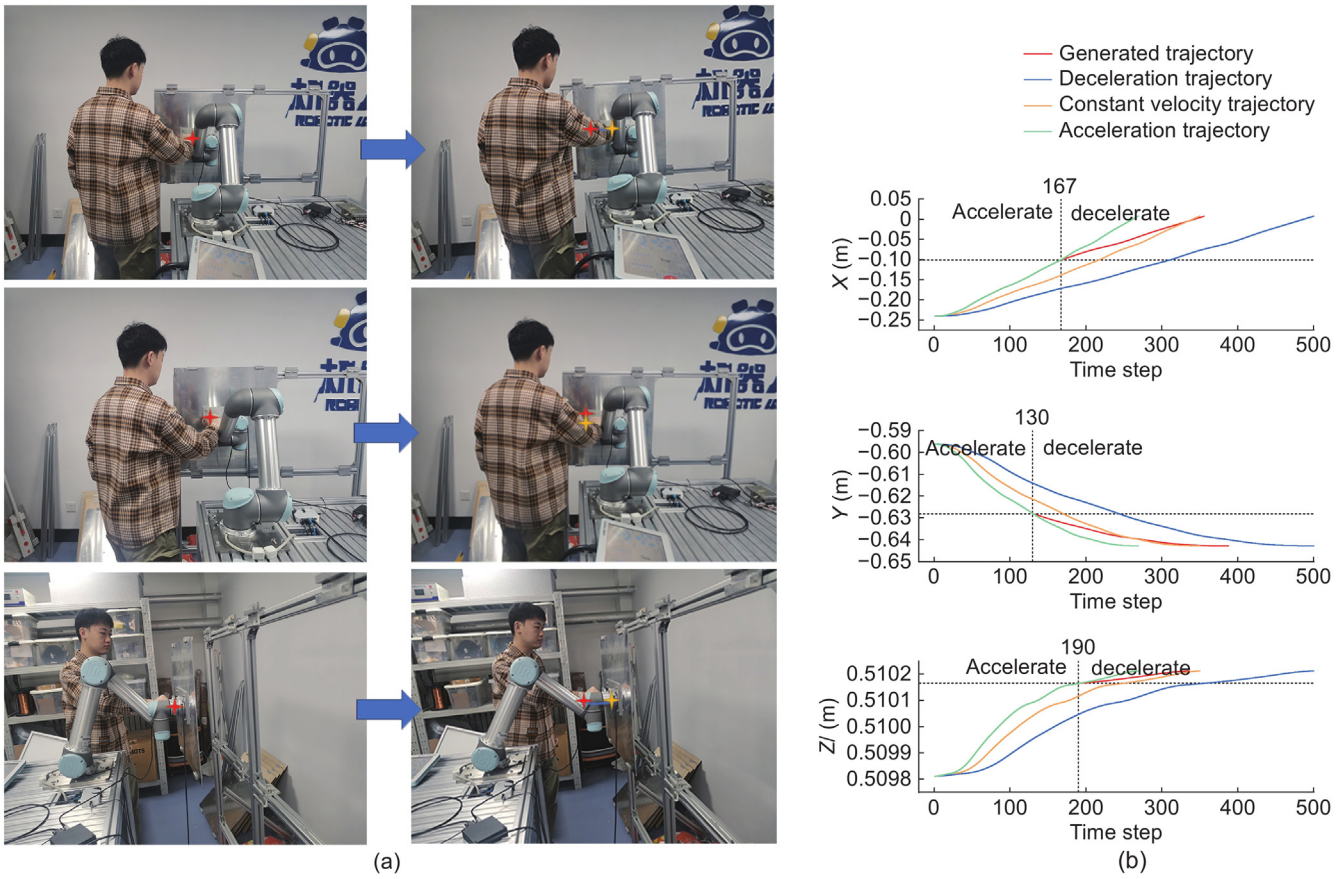

Fig. 10. Experiment for linear motion in space. (a) Diagram showing the experimental process. (b) Trajectory showing linear motion.

−0.27396, 0.24901) to the target point (0.07846, −0.42374, 0.34907). During the entire process of multiple accelerating and decelerating movements, there are three intentions to accelerate, 8 intentions to decelerate, and 7 intentions to maintain constant velocity in the simulation of the actual handling process. The experimental results are shown in Fig. 11.

During the experiment, the acceleration process is set time constant τ to 0.7, the deceleration process is set time constant τ to 1.3, and the constant speed process is set time constant τ to 1.0. By modifying the time parameter τ, the motion speed of the curtain wall is changed. According to an analysis of force, impulse, and speed, the human intention during the motion process is calculated. The green curve shown in the figure is related to human motion intention. The variable on the y-axis indicates the intention: a value of 1 represents an intention to accelerate, a value of 0 represents an intention to maintain constant speed, and a value of −1 represents an intention to decelerate. Through a real-time analysis of movement intention, trajectories for different speeds are selected, and the position of the next point is obtained based on the current position.

To provide a clearer representation of the accuracy of the motion of the robot guided by human intention, we use the Hausdorff distance between the final trajectory and the generalized trajectory to represent the trajectory error. The formula is expressed as Eq. (13):

$$h(A, B) = \max_{a \in A} \left\{ \min_{b \in B} \{ d(a, b) \} \right\} \tag{13}$$

where A and B are the final trajectory and the generalization trajectory, respectively. In this study, five human–machine collaborative processing experiments were carried out. The initial and end settings were the same for each experiment. The average trajectory error measured in the multidirectional spatial trajectory collaboration transport experiment was less than 0.00055 m, and the accuracy of the intention recognition was 100%. Therefore, the robot was able to identify the operator's intention and cooperate with the operator to carry out the handling of the curtain wall.

Traditional curtain wall handling requires at least three operators. The method proposed in this paper requires only one operator to conduct the intention guidance, and the handling task is carried out by the robot. The handling efficiency increases by more than 60% when the number of handlers is reduced from three to one, compared to the efficiency with three handlers.

5. Conclusions

This paper presents a collaborative handling system for curtain walls that leverages human intention understanding to enhance the robot handling skills. The system is designed around the "human–centered with machine support" concept, employing trajectory learning and generalization based on DMP to teach robot handling skills. By integrating human intention into the handling process, the proposed system effectively combines the strengths of both the robot and operator. This integration ensures a smooth, flexible, and labor-saving handling process, resulting in the accurate and safe completion of curtain wall tasks. Future research directions include optimizing the structure of the handling process to enhance the efficiency and improve the flexibility of robots in collaborative handling scenarios.

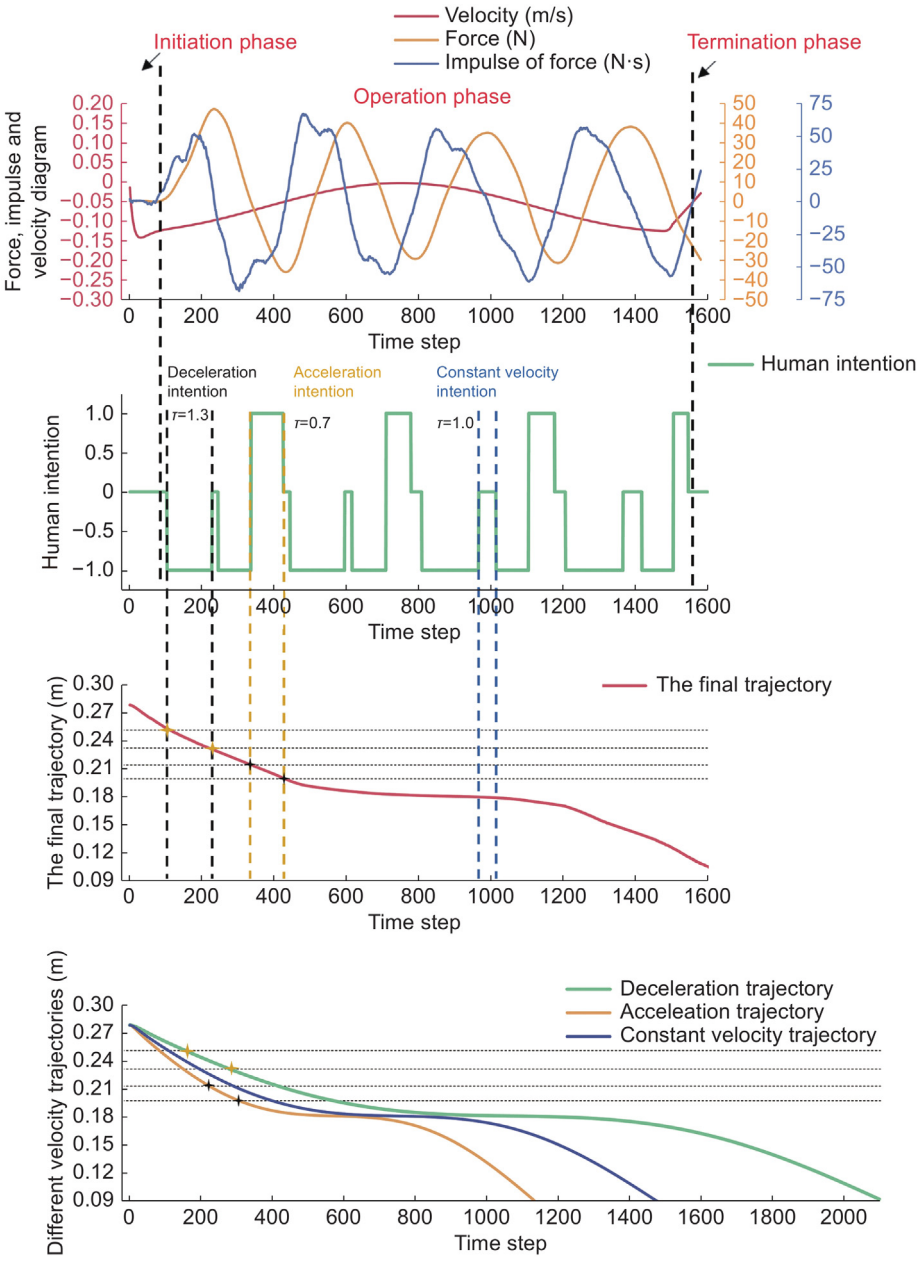

Fig. 11. Experiment for actual curtain wall handling.

CRediT authorship contribution statement

Fengming Li: Methodology, Funding acquisition, Conceptualization. **Huayan Sun:** Data curation. **Enguang Liu:** Project administration, Methodology, Conceptualization. **Fuxin Du:** Funding acquisition.

Declaration of competing interest

The authors declare that they have no known competing financial interests or personal relationships that could have appeared to influence the work reported in this paper.

Acknowledgments

This work was supported by 2022 Doctoral Fund Project of Shandong Jianzhu University (X22012Z) and the National Natural Science Foundation of China (U20A20283).

Appendix A. Supplementary data

Supplementary material related to this article can be found online at https://doi.org/10.1016/j.birob.2024.100183.

References

[1] S.N. Yu, S.Y. Lee, C.S. Han, K.Y. Lee, S.H. Lee, Development of the curtain wall installation robot: Performance and efficiency tests at a construction site, Auton. Robots 22 (2007) 281–291.

[2] H. Wu, W. Yan, Z. Xu, T. Cheng, A framework of robot skill learning from complex and long-horizon tasks, IEEE Trans. Autom. Sci. Eng. 19 (4) (2021) 3628–3638.

[3] O. Kroemer, S. Niekum, G. Konidaris, A review of robot learning for manipulation: Challenges, representations, and algorithms, J. Mach. Learn. Res. 22 (1) (2021) 1395–1476.

[4] J. Holas, I. Farkaš, Adaptive skill acquisition in hierarchical reinforcement learning, in: International Conference on Artificial Neural Networks, Springer International Publishing, Cham, 2020, pp. 383–394.

[5] J.M.D. Delgado, L. Oyedele, Robotics in construction: A critical review of the reinforcement learning and imitation learning paradigms, Adv. Eng. Inform. 54 (2022) 101787.
[6] Y. Hu, M. Cui, J. Duan, W. Liu, D. Huang, A. Knoll, G. Chen, Model predictive optimization for imitation learning from demonstrations, Robot. Auton. Syst. 163 (2023) 104381.
[7] A. Prados, S. Garrido, R. Barber, Learning and generalization of task-parameterized skills through few human demonstrations, Eng. Appl. Artif. Intell. 133 (2024) 108310.
[8] F. Iodice, Y. Wu, W. Kim, F. Zhu, D.M. Elena, A. Ajoudani, Learning cooperative dynamic manipulation skills from human demonstration videos, Mechatronics 85 (2022) 102807.
[9] Y. Shen, J. Wang, C. Feng, Q. Wang, Hybrid-driven autonomous excavator trajectory generation combining empirical driver skills and optimization, Autom. Constr. 165 (2024) 105523.
[10] Y. Shen, J. Wang, C. Feng, Y. Liu, D. Li, Y. Song, X. Qu, Jointly estimating the most likely driving paths and destination locations with incomplete vehicular trajectory data, Transp. Res. C 155 (2023) 104283.
[11] C. Liu, G. Peng, Y. Xia, J. Li, C. Yang, Robot skill learning system of multi-space fusion based on dynamic movement primitives and adaptive neural network control, Neurocomputing 574 (2024) 127248.
[12] W. Li, Y. Wang, Y. Liang, D.T. Pham, Learning from demonstration for autonomous generation of robotic trajectory: Status quo and forward-looking overview, Adv. Eng. Inform. 62 (2024) 102625.
[13] H. Zhao, Y. Chen, X. Li, H. Ding, Robotic peg-in-hole assembly based on reversible dynamic movement primitives and trajectory optimization, Mechatronics 95 (2023) 103054.
[14] L. Han, H. Yuan, W. Xu, Y. Huang, Modified dynamic movement primitives: robot trajectory planning and force control under curved surface constraints, IEEE Trans. Cybern. (2022).
[15] F. Yang, Q. Zheng, L. Chen, X. Tan, P. Che, Research on human behavior intention perception method based on wearable sensors, IEEE Access (2024).
[16] H.I. Lin, C.S.G. Lee, Speed-accuracy optimization for skill learning, in: 2009 IEEE International Conference on Robotics and Automation, IEEE, 2009, pp. 2506–2511.
[17] Q. Yang, C. Xie, R. Tang, H. Liu, R. Song, Hybrid active control with human intention detection of an upper-limb cable-driven rehabilitation robot, IEEE Access 8 (2020) 195206-195215.
[18] Y. Zhang, K. Ding, J. Hui, J. Lv, X. Zhou, P. Zheng, Human-object integrated assembly intention recognition for context-aware human–robot collaborative assembly, Adv. Eng. Inform. 54 (2022) 101792.
[19] Y. Pan, C. Chen, Z. Zhao, T. Hu, J. Zhang, Robot teaching system based on hand-robot contact state detection and motion intention recognition, Robot. Comput.-Integr. Manuf. 81 (2023) 102492.
[20] Z. Lu, N. Wang, M. Li, C. Yang, Incremental motor skill learning and generalization from human dynamic reactions based on dynamic movement primitives and fuzzy logic system, IEEE Trans. Fuzzy Syst. 30 (6) (2021) 1506–1515.